applied sciences

MDPI

Article

Aspect-Related Mechanical Properties of the Cortical Bone in the Third Metacarpal Bone of Mares

Bernard Turek [1], Grzegorz Mikułowski [2], Tomasz Szara [3], Michał Dołasiński [1], Tomasz Jasiński [1] and Małgorzata Domino [1,*]

[1] Department of Large Animal Diseases and Clinic, Institute of Veterinary Medicine, Warsaw University of Life Sciences (WULS–SGGW), 02-787 Warsaw, Poland; bernard_turek@sggw.edu.pl (B.T.); michal_dolasinski@sggw.edu.pl (M.D.); tomasz_jasinski@sggw.edu.pl (T.J.)
[2] Institute of Fundamental Technological Research, Polish Academy of Sciences (IPPT-PAN), 02-106 Warsaw, Poland; gmikulow@ippt.pan.pl
[3] Department of Morphological Sciences, Institute of Veterinary Medicine, Warsaw University of Life Sciences (WULS–SGGW), 02-787 Warsaw, Poland; tomasz_szara@sggw.edu.pl
* Correspondence: malgorzata_domino@sggw.edu.pl; Tel.: +48-22-59-36-191

Abstract: Complete fractures of the third metacarpal bone (MC III) diaphysis pose a significant clinical challenge, prompting advanced veterinary medicine to utilize constitutive and biomechanical modeling to better understand bone behavior. This study aims to compare the elastic modulus of the MC III cortical bone, supported by measurements of cortical bone thickness and relative density, across the dorsal, lateral, medial, and palmar aspects of the MC III, as well as to evaluate the cortical bone's response to compressive forces applied in different directions. Given the bone structure can exhibit sex-related differences, MC III bones were isolated from six equine cadaver limbs collected exclusively from mares and imaged using computed tomography (CT) to measure thickness and density. Cortical bone samples were collected from the four aspects of the MC III and subjected to mechanical testing followed by the elastic modulus calculation. Bone thickness and elastic modulus varied across the MC III aspects. Thinner cortical bone on the palmar aspect coincided with a lower sample reaction force-based elastic modulus in the externo-internal direction and a lower axial compression force elastic modulus in the proximo-distal direction. Regardless of the MC III aspect, the cortical bone demonstrated greater resistance to compressive forces when loaded in the vertical plane than in the horizontal plane. The returning of different values in mechanical tests depending on the direction of loading may be attributed to the anisotropic behavior of the cortical bone, which may implicate the increased risk of complete fractures of the MC III diaphysis due to a kick from another horse or a fall, rather than from training or competition-related overload.

Keywords: bone thickness; mechanical test; compression; bending; elastic modulus; equine

Academic Editor: Roger Narayan

Received: 21 December 2024
Revised: 1 February 2025
Accepted: 3 February 2025
Published: 5 February 2025

Citation: Turek, B.; Mikułowski, G.; Szara, T.; Dołasiński, M.; Jasiński, T.; Domino, M. Aspect-Related Mechanical Properties of the Cortical Bone in the Third Metacarpal Bone of Mares. *Appl. Sci.* **2025**, *15*, 1593. https://doi.org/10.3390/app15031593

1. Introduction

Fractures of the third metacarpal bone (MC III) in horses encompass a wide spectrum, ranging from marginal intra-articular fractures and condylar fractures to complete fractures of the diaphysis [1–5]. A significant proportion of MC III fractures are fatigue-related, often caused by improper training or overloading of the horse [6]. The first two types of fractures are relatively common, primarily affecting young racehorses [7], and generally do not pose major therapeutic challenges. Marginal fractures are typically treated arthroscopically [8], while simple condylar fractures are usually managed through osteosynthesis with screws

or screws and plates [3]. Both methods yield promising outcomes, often enabling horses to return to full performance following successful treatment [3,9,10]. In contrast, complete fractures of the MC III diaphysis are less common but present substantial therapeutic challenges for veterinarians [1,4,11,12]. These fractures are most frequently caused by kicks from other horses or falls [13] and often result in the euthanasia of the affected horses [14,15]. Consequently, efforts should focus on simulating bone behavior under physiological load and training [16,17], predicting bone overloading [18,19], and planning advanced surgical treatments for severe MC III fractures [12,19–23].

Progress in equine clinical practice could be significantly advanced through the development and application of constitutive and biomechanical modeling, such as the finite element method (FEM) [21,23]. FEM modeling can utilize slice geometry derived from computed tomography (CT) images to create accurate models of bone shapes [23]. With the increasing accessibility of CT imaging in equine clinical diagnostics [5], particularly with the advent of standing sedated CT examinations [24,25], using CT to model individual bone loads in horses represents a vital step forward in modern orthopedics. However, FEM simulations require specific experimental data on the mechanical properties of cortical and trabecular bones, such as elasticity, strength, and anisotropy, which directly influence the accuracy of stress, strain, and deformation predictions in the model. Without accurate experimental data, the simulation of the forces and loads acting on the equine skeleton may not reflect adequate bone behavior and thus theoretical clinical conditions [21].

Mechanical properties of bones are influenced by the direction of applied forces [26,27], as well as the architecture and composition of the bone, along with various individual and environmental factors [28–31]. Equine bone [26,32], as bovine [27,33,34] and human [33] bone, exhibits a typical anisotropic structure. Its structure, composition, and shape are affected by individual factors such as age and sex, as well as load-related factors, including body mass and the type and intensity of training [29,31]. Given the bone structure can exhibit differences related to age, sex, and body mass, this study was designed to investigate a consistent research group of female, mid-age and mid-size horses.

The mechanical properties of the entire MC III in horses, including its trabecular and cortical bone components, have been partially described [35–38]. However, to the best of our knowledge, no studies have specifically examined the elastic modulus of equine cortical bone at the mid-length of the diaphysis, a region prone to complete fractures of the MC III [1,3,13]. Given that the thickness of equine cortical bone varies significantly—from approximately 15 mm on the medial aspect of the mid-length diaphysis to about 5 mm on the lateral aspect of the distal metaphysis [23]—we hypothesized that the mechanical properties of cortical bone, and consequently the calculated elastic modulus, also vary depending on the aspect of the MC III. If confirmed, this aspect-related specificity of the elastic modulus could be incorporate into FEM research to enhance modeling of the geometrically complex equine MC III under theoretical clinical conditions [21], thereby improving training [16,17], overload prediction [18,19], and surgery planning [12,19–23].

The study aims to compare the elastic modulus, supported by measurements of cortical bone thickness and relative density, across the dorsal, lateral, medial, and palmar aspects of the MC III. Additionally, it seeks to evaluate the cortical bone's response to compressive forces applied in different directions.

2. Materials and Methods

2.1. Biological Samples

The prospective analytical study was conducted on six equine-isolated front limbs collected at the slaughterhouse. The inclusion criteria for enrolled horses were female sex, Warmblood bread, adult mid-age, and mid-size. The exclusion criteria included lameness

in the pre-mortem examination and the injuries—such as scars or wounds—visible in the metacarpal region. Limbs meeting the inclusion criteria were collected at the level of the carpometacarpal joint, creating a consistent research group characterized by adult female Warmblood horses of mid-age (median age = 7 years; range: 6–8 years) and mid-size (median weight = 575 kg; range: 550–600 kg). None of the horses were excluded due to the presence of lameness or signs of injury. Immediately after slaughter, limbs were placed at +4 °C and transported to the Equine clinic at the Warsaw University of Life Science. At the Equine clinic, limbs were imaged using CT following the protocol described in Section 2.2. The MC III were thoroughly cleaned of soft tissue, packed in individual plastic bags, and stored at −80 °C until mechanical testing described in Section 2.3, respectively.

From each bone, four samples were collected as shown on Figure 1. Thus, a total of 24 cortical bone samples were collected from the MC III after the bones had fully thawed a day before the expected date of the strength tests. Samples represented the dorsal, lateral, medial, and palmar aspect of the MC III bone, respectively. To ensure the repeatability of the bone sampling, cortical bone samples were taken from the geometrical center of bone determined individually in the mid-length of the diaphysis of each MC III. The samples were cut out using a diamond band pathology saw (Exact 312, EXAKT Advanced Technologies, Norderstedt, Germany) designed for bone processing. The speed of the cutting band ranged from 200 to 1200 m/min. The sampling process was cooled with water. The cut samples had a square base with sides of 80 × 80 mm, while side length was determined by the thickness of the cortical bone and ranged from 6 to 16 mm. From each bone sample, four cuboid samples with 5 mm sides were prepared. Each side of the cube was then marked to identify the surfaces and directions of force during mechanical testing. Such marking allowed for the compression test to be performed in the following three directions: the proximo-distal, externo-internal, and latero-lateral.

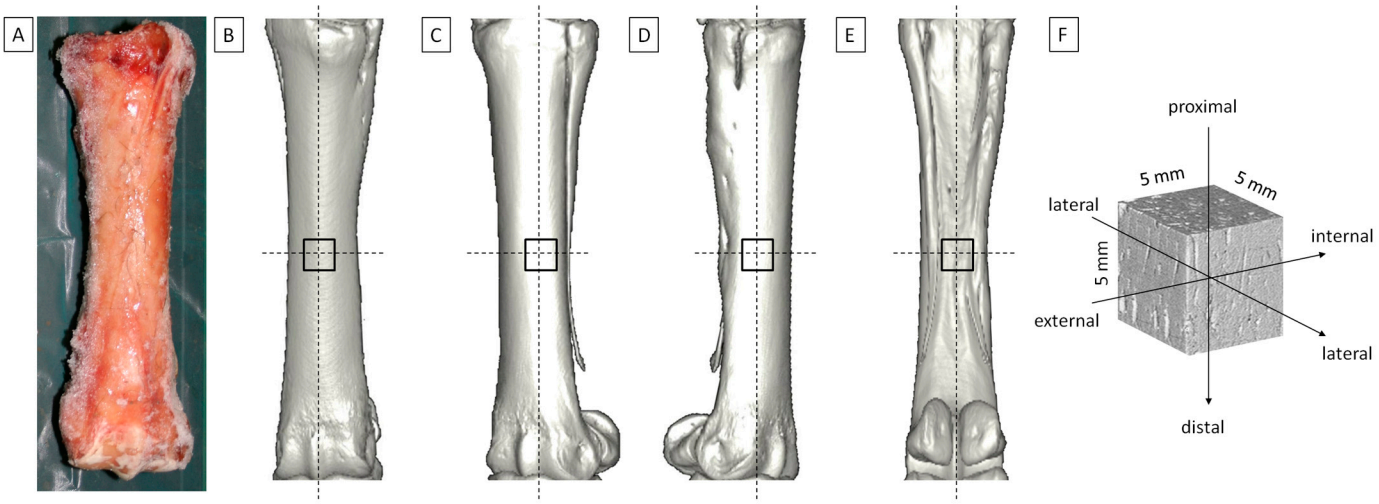

Figure 1. The metacarpal bone III (MC III) isolated from equine cadaver limb. (**A**) Frozen isolated MC III. Sampling sites of the cortical bone samples determined at the geometric center of each bone and representing (**B**) dorsal, (**C**) lateral, (**D**) medial, and (**E**) palmar aspects of the MC III, respectively. (**F**) Dimensions and directions of the cuboid sample of the cortical bone.

2.2. CT Imaging

The isolated limbs were imaged using a 64-slice CT scanner (Revolution CT, GE Healthcare, Chicago, IL, USA). The following imaging settings were used: a helical scan type; a current, 275 mA; a voltage, 120 kV; a gantry rotation, 0.08/s/HE+; a table travel, 39.4 mm/rotation; a pitch, 0.984:1; and a slice thickness, 0.625 mm. The scan length was adjusted between the carpometacarpal joint and the metacarpophalangeal joint to cover

the whole length of the MC III, and the number of slices was tailored to the limb's size. Images were saved in DICOM format using the AW workstation (GE Healthcare, Chicago, IL, USA) and Volume Share software version 7 (GE Healthcare, Chicago, IL, USA).

The DICOM files were displayed using Osirix MD software version 12.0 (Pixmeo SARL, Bernex, Switzerland) at the bone window (a level of +350 and a width of 2000). Cortical bone measurements were performed at the level of the geometrical center of the bone determined individually in the mid-length of the diaphysis of each MC III as shown in Figure 2A,B. All measurements were carried out on images in the axial plane. From each bone, four measurement lines were used to measure cortical bone thickness for the dorsal, lateral, medial, and palmar aspect of the MC III bone, separately (Figure 2C). The cortical bone thickness was measured as the longest distance between the bone surface and bone marrow cavity and reflected in mm. From each bone, four regions of interests (ROIs) were used to measure cortical bone relative density for the dorsal, lateral, medial, and palmar aspect of the MC III bone, separately (Figure 2D). The cortical bone relative density was a rectangle with a shorter side of 5.5 mm and a longer side adjusted to the bone thickness so that it covered only the cortical bone. The relative density was reflected in Hounsfield units (HUs). HU represents the radiodensity as −1000 for air, 0 HU for distilled water, 20–100 HU for soft tissue, up to 1000 HU for bone, and 2000 HU for dense bone or tooth [39].

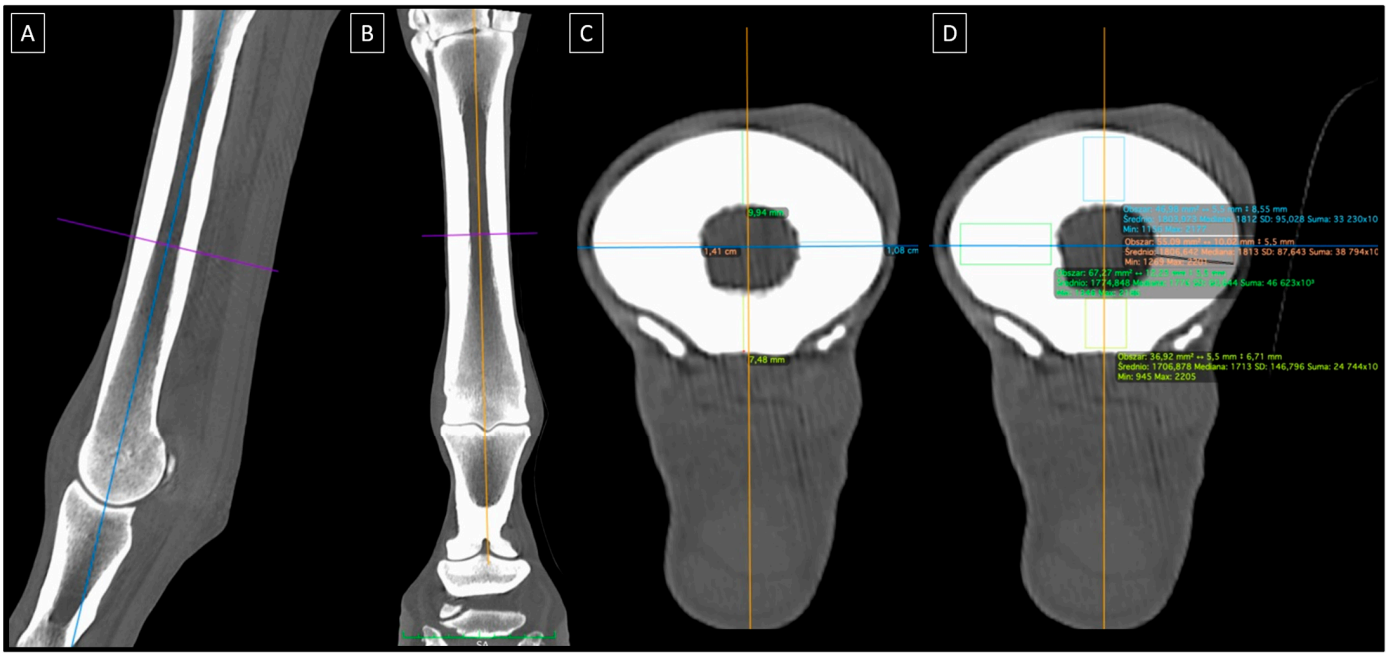

Figure 2. The metacarpal bone III (MC III) positioned on the computed tomography images in (**A**) sagittal, (**B**) coronal, and (**C**,**D**) axial plane. The measurement lines and regions of interests (ROIs) were determined at the geometric center of each bone. (**C**) Cortical bone thickness was measured using measurement lines, while (**D**) cortical bone relative density was measured using ROIs, on the dorsal, lateral, medial, and palmar aspects of the MC III, separately.

2.3. Mechanical Tests

Two mechanical tests were performed on the collected cortical bone samples—a 3-point bending test and a uniaxial compression test combined with a 2D DIC (Digital Image Correlation) technique to enhance data accuracy by providing full-field, non-contact strain measurements with high spatial resolution. The mechanical tests were performed using a servo-hydraulic MTS (Material Test System) machine equipped with two actuators. The first actuator (MTS 242.01) with a maximum force of 5 kN was equipped with a tensometric

force sensor with a measuring range of 5 kN and a LVDT piston rod displacement sensor with a range of 100 mm. The second actuator (MTS 244.12) with a maximum force of 25 kN was mounted in a vertical strength frame and equipped with a tensometric sensor with a measuring range of 25 kN, enabling the measurement of axial force. The first hydraulic actuator was used in the 3-point bending test, while the second hydraulic actuator was used in the uniaxial compression test combined with the DIC technique.

2.3.1. 3-Point Bending Test

In the 3-point bending test, samples were loaded in the external-internal direction. The distance between supports of 100 mm and a loading speed of 2 mm/min were used. The sample reaction force was recorded in the range of up to 1 kN and the deflection at the point of load application. The sample reaction force was interpreted as being counterbalanced with the external loading force and recorded. The test was terminated after the sample fracture. Based on the obtained measurement results, the elastic modulus of the cortical bone sample was calculated using Formula (1)

$$E = \frac{F}{u} \times \frac{L^3}{4bh^3} \quad (1)$$

where F is the force of loading the sample during the test, u is the maximum deflection arrow at the midpoint of the support spacing, L is distance between supports, b is the width of the sample cross-section at the point where the force was applied, and h is the height of the sample cross-section at the point where the force was applied [40].

2.3.2. Uniaxial Compression Test

In the uniaxial compression test, samples were loaded in three directions: the proximo-distal, externo-internal, and latero-lateral. A loading speed of 0.01 mm/s was used. The axial compression force was measured in the range of up to 25 kN and the deformation of the side wall of the sample was measured using the DIC technique. The measurement of the axial compression force was time-synchronized with the optical DIC measurement system. In the DIC technique, the optical device was equipped with an electronic module operating on the basis of the principle of digital 2D image correlation. The camera, set in the axis perpendicular to the cubic sample being tested, recorded a two-dimensional image at a frequency of 2 frames/s. Based on the recorded images, the deformation field on the surface of the samples was calculated in the elastic and plastic range. On the basis of the measured axial compression force and deflection of the samples, the stress and strain values were calculated, respectively. The test was carried out until 50% of the sample deformation was obtained. Based on the obtained measurement results, the elastic modulus of the cortical bone sample was calculated [41].

2.4. Statistical Analysis

The sample size was calculated based on data from a previous study [23] examining the thickness of equine cortical bone on the medial aspect of the mid-length diaphysis in the medial aspect (mean: 15 mm) and the lateral aspect (mean: 5 mm). Assuming a 95% significance level ($p \leq 0.05$), 80% study power, and 6.1 SD, the required sample size is 5.84. Thus, six isolated limbs were enrolled. Given that from each limb, four bone samples were collected for repeated measures, the data series, containing 24 realizations of each CT measurement and mechanical test, were tested for normality using the Kolmogorov–Smirnov normality test. Since not all data series followed a normal distribution, the data were presented in plots using medians and ranges (lower and upper quartiles, as well as

minimum and maximum values) as well as supported in the text by providing medians in parentheses.

Data series from each measurement/test were compared between assessed aspects of the MC III, while data series from a uniaxial compression test were compared between the directions of axial compression force acting. Data series were compared to paired data using the repeated measures ANOVA summary, when the normal distribution was confirmed for all compared data series, or Friedman test, when not normal distribution was confirmed for at least one compared data series. If significant differences were found in the first test, a post hoc test was performed. Repeated measures ANOVA summary was followed by Tukey's multiple comparisons test, while the Friedman test was followed by Dunn's multiple comparisons test. Statistical significance was set at $p < 0.05$.

Statistical analysis was performed using GraphPad Prism version 6 (GraphPad Software Inc., San Diego, CA, USA).

3. Results

3.1. Aspect-Related Properties of the MC III

Cortical bone thickness differed between aspects of the MC III ($p < 0.0001$). In the mid-length of the MC III diaphysis, the medial aspect (13.9 mm) was thicker than the dorsal (10.9 mm), lateral (10.9 mm), and palmar (6.6 mm) aspects, while the palmar aspect was thinner than the dorsal, lateral, and medial aspects. No significant difference in cortical bone thickness was found between the dorsal and lateral aspects of the MC III (Figure 3A). Moreover, cortical bone relative density did not vary significantly between aspects of the MC III (dorsal aspect, 1731 HU; lateral aspect, 1771 HU; medial aspect, 1724 HU; palmar aspect, 1698 HU; $p = 0.15$; Figure 3B).

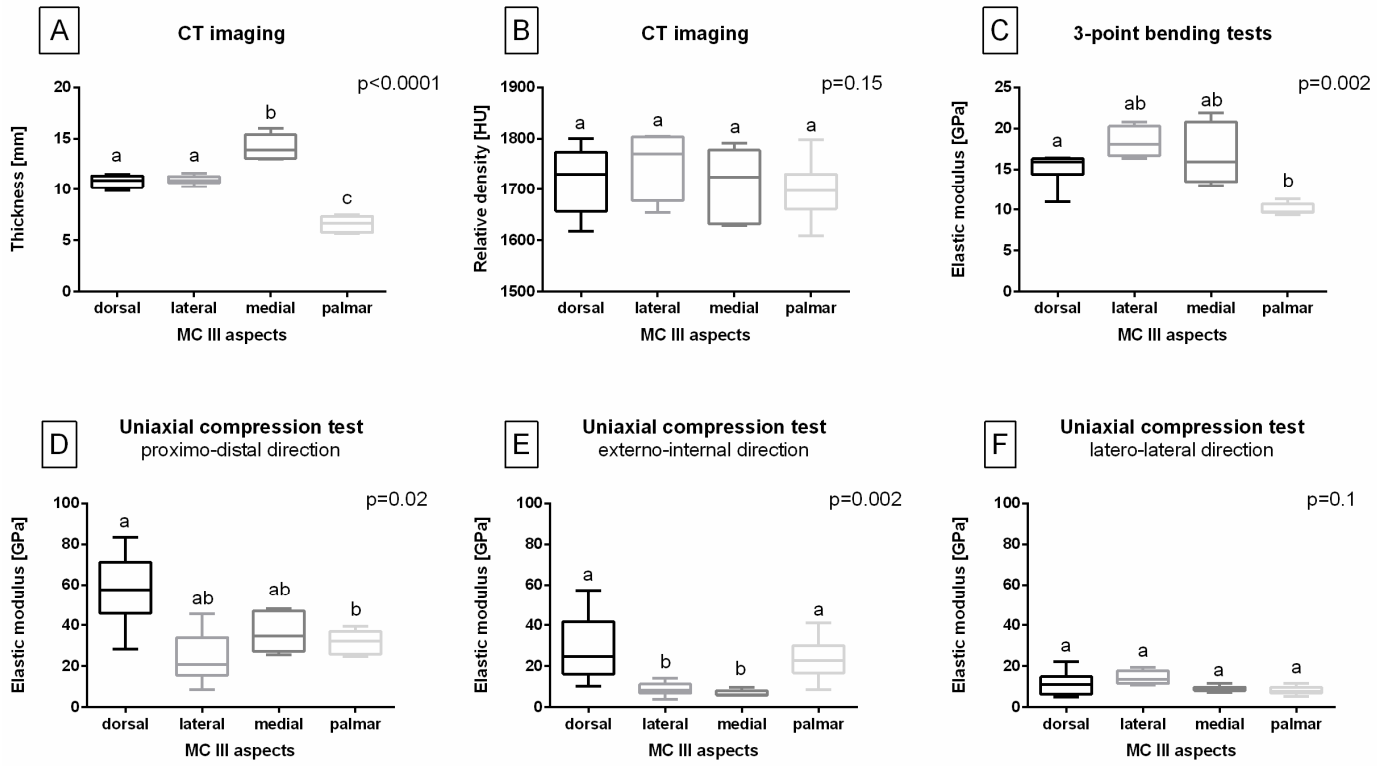

Figure 3. Aspect-related properties of the metacarpal bone III (MC III) include: (**A**) cortical bone thickness, (**B**) cortical bone relative density, and (**C**–**F**) the elastic modulus calculated based on the

results of mechanical tests. (**C**) The 3-point bending test in the external-internal direction; (**D**) uniaxial compression test in the proximo-distal direction; (**E**) uniaxial compression test in the external-internal direction; and (**F**) uniaxial compression test in the latero-lateral direction. Boxes represent lower quartile, median, and upper quartile, whereas whiskers represent minimum and maximum values. Lowercase letters (a, b, c) indicate significant differences between MC III aspects for $p < 0.05$.

The elastic modulus, calculated based on the sample reaction force from a 3-point bending test performed in the external-internal direction, differed between aspects of the MC III ($p = 0.002$). The sample reaction force-based elastic modulus was higher for the dorsal aspect (16.0 GPa) than for the palmar aspect (10.0 GPa), with no differences observed between the dorsal, lateral (18.1 GPa), and medial (16.0 GPa) aspects, or between the lateral, medial, and palmar aspects (Figure 3C).

The elastic modulus, calculated based on the axial compression force from the uniaxial compression test, differed between aspects of the MC III when tested in the proximo-distal direction ($p = 0.02$; Figure 3D) and the externo-internal direction ($p = 0.002$; Figure 3E) but not in the latero-lateral direction (dorsal aspect, 11.1 GPa; lateral aspect, 13.5 GPa; medial aspect, 8.9 GPa; palmar aspect, 7.9 GPa; $p = 0.1$; Figure 3F). In the proximo-distal direction, the axial compression force-based elastic modulus was higher for the dorsal aspect (57.5 GPa) than for the palmar aspect (32.4 GPa), with no differences observed between the dorsal, lateral (21.0 GPa), and medial (34.6 GPa) aspects, or between the lateral, medial, and palmar aspects. In the externo-internal direction, the axial compression force-based elastic modulus was higher for the dorsal (24.6 GPa) and palmar (22.7 GPa) aspects than for the lateral (8.3 GPa) and medial (6.2 GPa) aspects, with no differences observed between the dorsal and palmar aspects, or between the lateral and medial aspects.

It is notable that across all tested samples, the mean sample reaction force-based elastic modulus was 15.1 GPa (ranging from 9.4 to 21.9 GPa). However, due to the observed differences between MC III aspects, this value should not be generalized to the entire diaphysis.

3.2. Load Direction-Related Properties of the MC III

The elastic modulus, calculated based on the axial compression force from the uniaxial compression test, differed between tested directions in the dorsal ($p = 0.0007$; Figure 4A), lateral ($p = 0.04$; Figure 4B), medial ($p = 0.002$; Figure 4C), and palmar ($p = 0.004$; Figure 4D) aspects of the MC III. In the dorsal, lateral, and medial aspects, the elastic modulus was higher in the proximo-distal direction than in the externo-internal and latero-lateral directions, with no differences between the latter two. In the palmar aspect, the elastic modulus was highest in the proximo-distal direction, intermediate in the externo-internal direction, and lowest when in the latero-lateral direction.

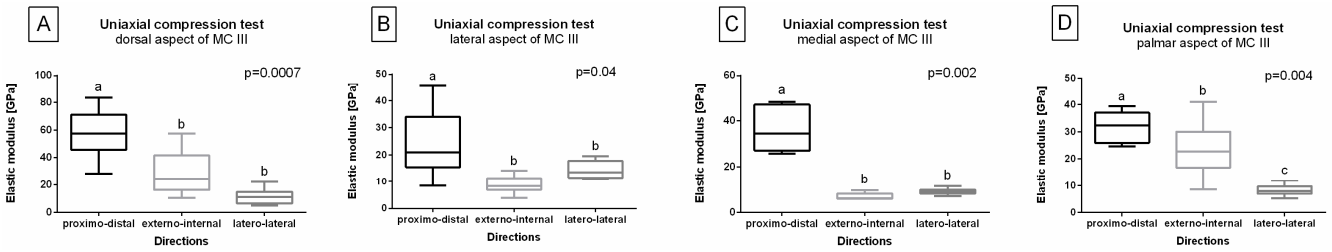

Figure 4. Load direction-related properties of the metacarpal bone III (MC III) include the elastic modulus calculated from the results of uniaxial compression test performed in the proximo-distal, external-internal direction, and latero-lateral directions. The axial compression force-based elastic modulus is compared across these tested directions for the (**A**) dorsal, (**B**) lateral, (**C**) medial, and

(**D**) palmar aspects of the MC III. Boxes represent lower quartile, median, and upper quartile, whereas whiskers represent minimum and maximum values. Lowercase letters (a, b, c) indicate significant differences between MC III aspects for $p < 0.05$.

Moreover, across all tested samples, the mean axial compression force elastic modulus was 37.4 GPa (ranging from 5.5 to 83.4 GPa) when tested in the proximo-distal direction and 17.0 GPa (ranging from 3.9 to 57.4 GPa) when tested in the externo-internal direction. However, due to the observed differences between MC III aspects, these values should not be generalized to the entire diaphysis. Additionally, the generalized mean axial compression force elastic modulus in the latero-lateral direction across all tested samples was 10.8 GPa (ranging from 4.9 to 22.3 GPa).

4. Discussion

The current study was designed to investigate the aspect-related mechanical properties of the cortical bone in MC III in a consistent research group. Therefore, only mares were included, as bone structure can exhibit sex-related differences [29,31]. Jackson et al. [29] reported sex-related variability in bone remodeling in racehorses, with males exhibiting higher levels of serum biomarkers for bone formation and resorption compared to females. De Oliveira Pereira et al. [31] found that the fractal dimension of the lateral aspect of the proximal phalanx was lower in males than in females, when they assessed bone radiographic texture. De Oliveira Pereira et al. [31] also highlighted age-related characteristics of equine trabecular bone in the proximal phalanx and MC III, showing an increase in bone fraction with age and training. However, to date, there are no reports on differences in the occurrence of complete fractures of the MC III diaphysis between mares, geldings, and stallions [13]. Therefore, the same generalization was ultimately applied when concluding equine predispositions to these fractures.

A comparison of the cross-sectional diaphysis of the MC III revealed that the cortical bone is thickest on the medial aspect and thinnest on the palmar aspect. The increased thickness of the cortical bone on the medial aspect of the forelimb is an adaptation to the natural loading of the limb during movement [16,17]. The forces acting on MC III along the long axis of the limb are greater than those acting in other directions due to the need to support a high body weight [42]. However, the resultant force on the MC III is a combination of forces acting along the limb's long axis and in the transverse and oblique forces. Non-vertical component forces are generated during limb abduction and are influenced by the horse's posture [43]. Non-vertical component forces subject the bone to bending in the dorsal and sagittal planes, particularly in the externo-internal and latero-lateral directions [44–47]. This effect is especially relevant since many horses exhibit a toe-out and adducted thoracic posture rather than a completely straight posture [43,48]. Although non-vertical component forces are much smaller than the vertical forces acting in the proximal-distal direction [44–47], they may contribute to the remodeling of the equine cortical bone [49].

The current results support the hypothesis that the mechanical properties of cortical bone vary depending on the aspect of the MC III, confirming the aspect-related specificity of the elastic modulus. Therefore, a single elastic modulus should not be generalized to the entire MC III diaphysis, and aspect-specific cortical bone properties should be incorporated into future FEM models. This improvement may enhance the modeling of MC III [21] for various clinical applications, such as training optimization [16,17], overload prediction [18,19], and surgical planning—particularly for advanced surgical treatments of complete MC III fractures [12,19–23]. Notably, the thinner cortical bone on the palmar aspect of the MC III coincides with a lower sample reaction force-based elastic modulus and a lower axial compression force-based elastic modulus in the proximo-distal direction.

Interestingly, no differences in relative bone density were observed between the studied aspects, suggesting that the reduced bending and compression strength on the palmar aspect of the MC III may be attributed to the thinner cortical bone. However, this hypothesis requires further investigation involving a larger cohort of horses. The current results partially align with those reported by Les et al. [50], who documented the highest values of Young's modulus of elasticity for the lateral and medial aspects of the equine MC III, followed by the dorsal and palmar aspects. It is worth noting that their study only involved a compression test of cylindrical samples loaded in the proximo-distal direction [50]. However, neither the intermediate thickness of the dorsal aspect of the MC III nor previous studies account for the greater strength of the dorsal aspect observed in this study for bending in the externo-internal direction and compression in both the externo-internal and proximo-distal directions.

It is important to note that in the discussed 3-point bending test, cortical bone samples were subjected to force in the externo-internal direction. However, the compression-force-based elastic modulus in the externo-internal direction was higher in the palmar and dorsal aspects compared to the lateral and medial aspects. The observed differences in bending and compression strength, even when the force acts in the same direction, may be attributed to bone anisotropy [26,27,32]. Cortical bone is highly anisotropic with a non-homogeneous morphological structure. Therefore, it returns different values in mechanical tests depending on the direction of loading [27,50]. Different aspect-related values in mechanical tests, depending on the direction of loading, may have clinical implications, suggesting an increased risk of complete fractures of the MC III diaphysis due to kicks from other horses or falls, rather than from training or competition-related overload. The equine MC III bone can withstand the greatest loads in the proximo-distal direction [42], which aligns with the orientation of fibers in the extracellular matrix (ECM) of cortical bone, a factor that significantly influences bone strength parameters [26,27,32]. Additionally, the properties of cortical bone differ depending on the type of loading (i.e., bending vs. compression). This highlights the need for further investigation of the cortical bone structure using μCT [30,51] and bone composition analysis using the computed digital absorptiometry (CDA) [52,53], dual energy x-ray absorptiometry (DEXA) [52,54], or dual energy computed tomography (DE CT) [55]. These studies could help explain the variations in bone response to different forces (the sample reaction force and the axial compression force) in the same direction, as well as the similarities in bone response to different forces applied in different directions.

In the discussed 3-point bending test, the externo-internal direction of forces acting was chosen to study the bending of the cortical bone because it aligns with the primary cause for the MC III fractures. These include being kicked by another horse or falling during training or competitions like show jumping or eventing [1,3,13], where the force typically acts horizontally to the ground, and which are the most common causes of complete fractures of the MC III diaphysis in horses [1–5,12,22]. Comparison of the axial compression force-based elastic modulus across the tested directions revealed that, regardless of the MC III aspect, the cortical bone is more resistant to compression when the force acts in the proximo-distal direction compared to the externo-internal or latero-lateral directions. This finding aligns with the results of Biewener et al. [42], which indicated that the equine skeleton is primarily loaded by compression, and with the observation by Bonfield and Grynpa [34] that changing the loading direction from proximo-distal to latero-lateral influences the value of the elastic modulus. However, it should be noted that Bonfield and Grynpa's study investigated bovine, not equine, cortical bone [34]. Additionally, Reilly and Burstain [33] showed that in bovine and human cortical bone, the Young's modulus of elasticity is more than twice as great for proximo-distal loading compared to externo-internal or latero-lateral

loading. The translation of these findings from bovine to equine bone, along with the current results, may provide new insights into why an equine healthy MC III bone does not frequently fracture upon landing after jumping over an obstacle [25] but may fracture after being kicked or from a fall [1,3,13].

The limitation of this study is the small sample size. Although the number of individual sections met the minimum criteria for group analysis [56], the results should be considered preliminary. Despite the limited sample size, significant differences in the thickness and mechanical properties of the cortical bone at the mid-length of the MC III diaphysis were identified. As this study was designed on female individuals, further research is needed on a larger cohort of horses to establish the effect of horse sex, age, breed, and usage on the mechanical behavior of MC III [16,28–31]. Additionally, when considering the elastic modulus calculated from the 3-point bending test and the uniaxial compression test, the observed variability in results, as reflected by the wide ranges, is notable. This variability was present across all tested aspects of the MC III and all tested directions of the applied axial compression force. It may also be a consequence of a focal observation of the forces as, in the natural loading of the limb, all aspects of the MC III receive forces during movement. Thus, the dissipation and absorption of forces, as well as the bone's response to them, should be further considered. Expanding the study to include a larger sample size would improve the reliability of these estimations. Another limitation of this study is the lack of tensile tests, which are important due to the role of ECM in providing strength to the cortical bone [27]. Since the direction of ECM fibers [26,27,32] and the content of mineral [37,38] substances significantly affect the mechanical properties of bone, further studies should incorporate three mechanical tests—bending, compression, and tensile tests—examined in three directions. Additionally, assessments of bone architecture using μCT [30,37,51] and hydroxyapatite content through DE CT studies [55] would provide valuable insights into the properties of subsequent aspects of the MC III. Such data could enhance the experimental data for the FEM analysis and their applications like simulating bone behavior under physiological load and training [16,17], predicting bone overloading [18,19], and planning surgical treatments [12,19–23], ultimately contributing to advancements in equine clinical practice.

5. Conclusions

Cortical bone thickness and elastic modulus varied across aspects of the MC III at the mid-length of the diaphysis. Due to non-generalizable elastic modulus values, aspect-specific cortical bone properties should be incorporated into future FEM modeling for clinical applications, including training monitoring, fracture risk prediction, and treatment planning. The thinner cortical bone on the palmar aspect of the MC III co-occurred with a lower sample reaction force-based elastic modulus in the externo-internal direction and a lower axial compression force elastic modulus in the proximo-distal direction. However, the thicker cortical bone on the medial aspect of the MC III did not co-occur with superior mechanical properties. In contrast, the dorsal aspect of the MC III exhibited increased bending and compression strength when loaded in both the proximo-distal and externo-internal directions. Regardless of the MC III aspect, the cortical bone demonstrated greater resistance to compression forces when loaded along the axial direction of the limb compared to the horizontal plane. This may predispose horses to complete fractures of the MC III diaphysis following a kick from another horse or a fall. The findings of this study should be considered preliminary, underscoring the need for further research to establish reference values for the elastic modulus, which could be utilized in numerical simulations to support advanced procedures in the equine practice.

Author Contributions: Conceptualization, B.T. and M.D. (Małgorzata Domino); methodology, B.T., G.M., T.J. and M.D. (Małgorzata Domino); software, B.T., G.M., T.J. and M.D. (Małgorzata Domino); validation, B.T. and T.J.; formal analysis, B.T., G.M. and M.D. (Małgorzata Domino); investigation, B.T., G.M., T.S., M.D. (Michał Dołasiński), T.J. and M.D. (Małgorzata Domino); resources, B.T., G.M. and T.J.; data curation, B.T.; writing—original draft preparation, B.T., G.M., M.D. (Michał Dołasiński) and M.D. (Małgorzata Domino); writing—review and editing, B.T., G.M., T.S., M.D. (Michał Dołasiński), T.J. and M.D. (Małgorzata Domino); visualization, B.T. and M.D. (Małgorzata Domino); supervision, M.D. (Małgorzata Domino); project administration, B.T. All authors have read and agreed to the published version of the manuscript.

Funding: This research received no external funding.

Institutional Review Board Statement: The research, using the samples collected postmortem at a commercial slaughterhouse, does not fall under the legislation for the protection of animals used for scientific purposes, national decree-law (Dz. U. 2015 poz. 266 and 2010-63-EU directive). No ethical approval was needed.

Informed Consent Statement: Not applicable.

Data Availability Statement: The data presented in this study are available upon request from the corresponding author.

Conflicts of Interest: The authors declare no conflicts of interest.

References

1. Bischofberger, A.S.; Fürst, A.; Auer, J.; Lischer, C. Surgical management of complete diaphyseal third metacarpal and metatarsal bone fractures: Clinical outcome in 10 mature horses and 11 foals. *Equine Vet. J.* **2009**, *41*, 465–473. [CrossRef] [PubMed]
2. Bogers, S.H.; Rogers, C.W.; Bolwell, C.; Roe, W.; Gee, E.; McIlwraith, C.W. Quantitative comparison of bone mineral density characteristics of the distal epiphysis of third metacarpal bones from Thoroughbred racehorses with or without condylar fracture. *Am. J. Vet. Res.* **2016**, *77*, 32–38. [CrossRef]
3. Moulin, N.; François, I.; Coté, N.; Alford, C.; Cleary, O.; Desjardins, M.R. Surgical repair of propagating condylar fractures of the third metacarpal/metatarsal bones with cortical screws placed in lag fashion in 26 racehorses (2007–2015). *Equine Vet. J.* **2018**, *50*, 629–635. [CrossRef] [PubMed]
4. Lischer, C.; Klaus, C. Diaphyseal fractures of the Third Metacarpal and Third Metatarsal Bones. In *Fractures in the Horse*; Wiley: Hoboken, NJ, USA, 2022.
5. Steel, C.; Ahern, B.; Zedler, S.; Vallance, S.; Galuppo, L.; Richardson, J.; Whitton, C.; Young, A. Comparison of Radiography and Computed Tomography for Evaluation of Third Carpal Bone Fractures in Horses. *Animals* **2023**, *13*, 1459. [CrossRef]
6. Morgan, R.; Dyson, S. Incomplete longitudinal fractures and fatigue injury of the proximopalmar medial aspect of the third metacarpal bone in 55 horses. *Equine Vet. J.* **2012**, *44*, 64–70. [CrossRef] [PubMed]
7. Reardon, R.J.; Boden, L.; Stirk, A.J.; Parkin, T.D.H. Accuracy of distal limb fracture diagnosis at British racecourses 1999–2005. *Vet. Rec.* **2014**, *174*, 477. [CrossRef]
8. Wright, I.M.; Nixon, A.J. Fractures of the condyles of the third metacarpal and metatarsal bones. In *Equine Fracture Repair*; Wiley: Hoboken, NJ, USA, 2019.
9. Misheff, M.M.; Alexander, G.R.; Hirst, G.R. Management of fractures in endurance horses. *Equine Vet. Educ.* **2010**, *22*, 623–630. [CrossRef]
10. Young, N.; Corletto, F.; Wright, I. Predicting return to racing after repair of fractures of the metacpal/metatarsal condyles in Thoroughbred racehorses. *Vet. Surg.* **2022**, *51*, 753–762. [CrossRef] [PubMed]
11. McClure, S.R.; Watkins, J.P.; Glickman, N.W.; Hawkins, J.F.; Glickman, L.T. Complete fractures of the third metacarpal or metatarsal bone in horses: 25 cases (1980–1996). *J. Am. Vet. Med. Assoc.* **1998**, *213*, 847–850. [CrossRef]
12. Turek, B.; Potyński, A.; Wajler, C.; Szara, T.; Czopowicz, M.; Drewnowska, O. Biomechanical study in vitro on the use of self-designed external fixator in diaphyseal III metacarpal fractures in horses. *Pol. J. Vet. Sci.* **2015**, *18*, 323–332. [CrossRef]
13. Donati, B.; Fürst, A.E.; Hässig, M.; Jackson, M.A. Epidemiology of fractures: The role of kick injuries in equine fractures. *Equine Vet. J.* **2018**, *50*, 580–586. [CrossRef] [PubMed]
14. Sarrafian, T.L.; Case, J.T.; Kinde, H.; Daft, B.M.; Read, D.H.; Moore, J.D.; Stover, S.M. Fatal musculo-skeletal injuries of Quarter Horse racehorses: 314 cases (1990–2007). *J. Am. Vet. Med. Assoc.* **2012**, *241*, 935–942. [CrossRef]
15. Springer, S.; Jenner, F.; Tichy, A.; Grimm, H. Austrian veterinarians' attitudes to euthanasia in equine practice. *Animals* **2019**, *9*, 44. [CrossRef] [PubMed]

16. Harrison, S.M.; Whitton, R.C.; Kawcak, C.E.; Stover, S.M.; Pandy, M.G. Evaluation of a subject-specific finite-element model of the equine metacarpophalangeal joint under physiological load. *J. Biomech.* **2014**, *47*, 65–73. [CrossRef] [PubMed]
17. Shaktivesh, S.; Malekipour, F.; Whitton, R.C.; Hitchens, P.L.; Lee, P.V. Fatigue behavior of subchondral bone under simulated physiological loads of equine athletic training. *J. Mech. Behav. Biomed. Mater.* **2020**, *110*, 103920. [CrossRef] [PubMed]
18. McCarty, C.A.; Thomason, J.J.; Gordon, K.D.; Burkhart, T.A.; Milner, J.S.; Holdsworth, D.W. Finite-element analysis of bone stresses on primary impact in a large-animal model: The distal end of the equine third metacarpal. *PLoS ONE* **2016**, *11*, e0159541. [CrossRef]
19. Słowiński, J.; Roszak, M.; Krawiec, K.; Henklewski, R.; Jamroziak, K. Numerical Analysis of Stabilization of a Horse's Third Metacarpal Bone Fracture for Prediction of the Possibility of Bone Union. *Appl. Sci.* **2024**, *14*, 7976. [CrossRef]
20. Lescun, T.B.; McClure, S.R.; Ward, M.P.; Downs, C.; Wilson, D.A.; Adams, S.B.; Hawkins, J.F.; Reinertson, E.L. Evaluation of transfixation casting for treatment of third metacarpal, third metatarsal, and phalangeal fractures in horses: 37 cases (1994–2004). *J. Am. Vet. Med. Assoc.* **2007**, *230*, 1340–1349. [CrossRef] [PubMed]
21. Brianza, S.; Brighenti, V.; Lansdowne, J.L.; Schwieger, K.; Bouré, L. Finite element analysis of a novel pin-sleeve system for external fixation of distal limb fractures in horses. *Vet. J.* **2011**, *190*, 260–267. [CrossRef] [PubMed]
22. Turek, B.; Potyński, A.; Drewnowska, O. Own-design external fixator for the treatment of diaphyseal fractures of the third metacarpal bone in horses. *Med. Weter.* **2016**, *72*, 197–202.
23. Lescun, T.B.; Adams, S.B.; Main, R.P.; Nauman, E.A.; Breur, G.J. Finite Element Analysis of Six Transcortical Pin Parameters and Their Effect on Bone–Pin Interface Stresses in the Equine Third Meta-carpal Bone. *Vet. Comp. Orthop. Traumatol.* **2020**, *33*, 121–129. [CrossRef] [PubMed]
24. Nagy, A.; Boros, K.; Dyson, S. Magnetic resonance imaging, computed tomographic and radiographic findings in the metacarpophalangeal joints of 40 non-lame Thoroughbred Yearlings. *Animals* **2023**, *13*, 3466. [CrossRef]
25. Nagy, A.; Dyson, S. Magnetic Resonance Imaging, Computed Tomographic and Radiographic Findings in the Metacarpophalangeal Joints of 31 Warmblood Showjumpers in Full Work and Competing Regularly. *Animals* **2024**, *14*, 1417. [CrossRef]
26. Skedros, J.G.; Dayton, M.R.; Sybrowsky, C.L.; Bloebaum, R.D.; Bachus, K.N. The influence of collagen fiber orientation and other histocompositional characteristics on the mechanical properties of equine cortical bone. *J. Exp. Biol.* **2006**, *209*, 3025–3042. [CrossRef] [PubMed]
27. Novitskaya, E.; Chen, P.-Y.; Lee, S.; Castro-Ceseña, A.; Hirata, G.; Lubarda, V.A.; McKittrick, J. Anisotropy in the compressive mechanical properties of bovine cortical bone and the mineral and protein constituents. *Mater. Sci. Eng.* **2011**, *7*, 3170–3177. [CrossRef]
28. Glade, M.J.; Luba, N.K.; Schryver, H.F. Effects of age and diet on the development of mechanical strength by the third metacarpal and metatarsal bones of young horses. *J. Anim. Sci.* **1986**, *63*, 1432–1444. [CrossRef]
29. Jackson, B.F.; Lonnell, C.; Verheyen, K.; Wood, J.L.N.; Pfeiffer, D.U.; Price, J.S. Gender differences in bone turnover in 2-year-old horses. *Equine Vet. J.* **2014**, *46*, 303–310.
30. Marsiglia, M.F.; Yamada, A.L.M.; Agreste, F.R.; de Sá, L.R.M.; Nieman, R.T.; da Silva, L.C.L.C. Morphological analysis of third metacarpus cartilage and subchondral bone in Thoroughbred racehorses: An ex vivo study. *Anat. Rec.* **2022**, *305*, 3385–3397. [CrossRef]
31. de Oliveira Pereira, L.; de Souza, A.F.; Yamada, A.L.M.; de Andrade Salgado, D.R.; De Zoppa, A.L.D.V. Radiographic Texture of the Trabecular Bone in the Proximal Phalanx of Horses. *Int. J. Equine Sci.* **2024**, *3*, 107–114.
32. Rho, J.Y.; Currey, J.D.; Zioupos, P.; Pharr, G.M. The anisotropic Young's modulus of equine secondary osteones and interstitial bone determined by nanoindentation. *J. Exp. Biol.* **2001**, *204*, 1775–1781. [CrossRef] [PubMed]
33. Reilly, D.T.; Burstein, A.H. The elastic and ultimate properties of compact bone tissue. *J. Biomech.* **1975**, *8*, 393–405. [CrossRef] [PubMed]
34. Bonfield, W.; Grynpas, M.D. Anisotropy of the Young's modulus of bone. *Nature* **1977**, *270*, 453–454. [CrossRef] [PubMed]
35. Les, C.M.; Keyak, J.H.; Stover, S.M.; Taylor, K.T.; Kaneps, A.J. Estimation of material properties in the equine metacarpus with use of quantitative computed tomography. *J. Orthop. Res.* **1994**, *12*, 822–833. [CrossRef]
36. Rubio-Martínez, L.M.; Cruz, A.M.; Gordon, K.; Hurtig, M.B. Mechanical properties of subchondral bone in the distal aspect of third metacarpal bones from Thoroughbred racehorses. *Am. J. Vet. Res.* **2008**, *69*, 1423–1433. [CrossRef] [PubMed]
37. Leahy, P.D.; Smith, B.S.; Easton, K.L.; Kawcak, C.E.; Eickhoff, J.C.; Shetye, S.S.; Puttlitz, C.M. Correlation of mechanical properties within the equine third metacarpal with trabecular bending and multi-density micro-computed tomography data. *Bone* **2010**, *46*, 1108–1113. [CrossRef] [PubMed]
38. Symons, J.E.; Entwistle, R.C.; Arens, A.M.; Garcia, T.C.; Christiansen, B.A.; Fyhrie, D.P.; Stover, S.M. Mechanical and morphological properties of trabecular bone samples obtained from third metacarpal bones of cadavers of horses with a bone fragility syndrome and horses unaffected by that syndrome. *Am. J. Vet. Res.* **2012**, *73*, 1742–1751. [CrossRef] [PubMed]
39. Hounsfield, G.N. Nobel Award address. Computed medical imaging. *Med. Phys.* **1980**, *7*, 283–290. [CrossRef] [PubMed]

40. Keller, T.S.; Mao, Z.; Spengler, D.M. Young's modulus, bending strength, and tissue physical properties of human compact bone. *J. Orthop. Res.* **1990**, *8*, 592–603. [CrossRef]
41. Odgaard, A.; Linde, F. The underestimation of Young's modulus in compressive testing of cancellous bone specimens. *J. Biomech.* **1991**, *24*, 691–698. [CrossRef]
42. Biewener, A.A. Allometry of quadrupedal locomotion: The scaling of duty factor, bone curvature, and limb orientation to body size. *J. Exp. Biol.* **1983**, *105*, 147–171. [CrossRef] [PubMed]
43. Shahkhosravi, N.A.; Bellenzani, M.C.; Davies, H.M.; Komeili, A. The influence of equine limb conformation on the biomechanical responses of the hoof: An in vivo and finite element study. *J. Biomech.* **2021**, *128*, 110715. [CrossRef]
44. Barnes, G.; Pinder, D. In-vivo tendon tension and bone strain measurement and correlation. *J. Biomech.* **1974**, *7*, 35–42. [CrossRef] [PubMed]
45. Gross, T.S.; McLeod, K.J.; Rubin, C.T. Technical note: Characterizing bone' strain distributions in vivo using three triple rosette strain gages. *J. Biomech.* **1992**, *25*, 1081–1087. [CrossRef] [PubMed]
46. Rybicki, E.; Mills, E.; Turner, A.; Simonen, F. In vivo and analytical studies of forces and moments in equine long bone. *J. Biomech.* **1977**, *10*, 701–705. [CrossRef] [PubMed]
47. Turner, A.; Mills, E.; Gabel, A. In vivo measurement of bone strain in the horse. *Am. J. Vet. Res.* **1975**, *36*, 1573–1579.
48. Sauer, F.J.; Hellige, M.; Beineke, A.; Geburek, F. Osteoarthritis of the coxofemoral joint in 24 horses: Evaluation of radiography, ultrasonography, intra-articular anesthesia, treatment, and outcome. *Equine Vet. J.* **2024**, *57*, 101–104. [CrossRef]
49. Wang, X.; Thomas, C.D.L.; Clement, J.G.; Das, R.; Davies, H.; Fernandez, J.W. A mechanostatistical approach to cortical bone remodelling: An equine model. *Biomech. Model. Mechanobiol.* **2016**, *15*, 29–42. [CrossRef] [PubMed]
50. Les, C.M.; Stover, S.M.; Keyak, J.H.; Taylor, K.T.; Willits, N.H. The distribution of material properties in the equine third metacarpal bone serves to enhance sagittal bending. *J. Biomech.* **1997**, *30*, 355–361. [CrossRef] [PubMed]
51. Oliviero, S.; Giorgi, M.; Dall'Ara, E. Validation of finite element models of the mouse tibia using digital volume correlation. *J. Mech. Behav. Biomed. Mater.* **2018**, *86*, 172–184. [CrossRef] [PubMed]
52. Bowen, A.J.; Burd, M.A.; Craig, J.J.; Craig, M. Radiographic calibration for analysis of bone mineral density of the equine third metacarpal bone. *J. Equine Vet. Sci.* **2013**, *33*, 1131–1135. [CrossRef]
53. Turek, B.; Borowska, M.; Jankowski, K.; Skierbiszewska, K.; Pawlikowski, M.; Jasiński, T.; Domino, M. A Preliminary Protocol of Radiographic Image Processing for Quantifying the Severity of Equine Osteoarthritis in the Field: A Model of Bone Spavin. *Appl. Sci.* **2024**, *14*, 5498. [CrossRef]
54. McClure, S.R.; Glickman, L.T.; Glickman, N.W.; Weaver, C.M. Evaluation of dual-energy x-ray absorptiometry for in situ measurement of bone mineral density of equine metacarpi. *Am. J. Vet. Res.* **2001**, *62*, 752–756. [CrossRef] [PubMed]
55. Skierbiszewska, K.; Szałaj, U.; Turek, B.; Sych, O.; Jasiński, T.; Łojkowski, W.; Domino, M. Radiological properties of nano-hydroxyapatite compared to natural equine hydroxyapatite quantified using dual-energy CT and high-field MR. *Nanomedicine* **2024**, *61*, 102765. [CrossRef]
56. Charan, J.; Kantharia, N. How to calculate sample size in animal studies. *J. Pharmacol. Pharmacother.* **2013**, *4*, 303–306. [CrossRef]